Receiver Component Evaluation for an Optical MIMO Testbed

Heidi Köhnke[1], Andreas Ahrens[2], Steffen Lochmann[3]

Hochschule Wismar, University of Technology, Business and Design,
Philipp-Müller-Straße 14, 23966 Wismar, Germany
[1]h.koehnke@stud.hs-wismar.de, [2]andreas.ahrens@hs-wismar.de,
[3]steffen.lochmann@hs-wismar.de

Abstract

Within the last years the interest in methods of optical multiple-input multiple-output (MIMO) transmission has increased significantly. To investigate the effects in a transmission system, an optical MIMO testbed has been set up. The measured data are used to develop a testbed-related (2×2) optical MIMO system model. Focus of this work is on the development and testing of various MATLAB/Simulink-based receiver implementations for an optical (2×2) MIMO testbed. The successful implementation of the various receiver components is shown by the eye diagram.

1 Introduction

The growing demand on bandwidth particularly driven by the developing Internet has been satisfied so far by optical fibre technologies such as Dense Wavelength Division Multiplexing (DWDM), Polarization Multiplexing (PM) and multi-level modulation. These technologies have now reached a state of maturity [1]. The only way to further increase the available data rate is now seen in the area of spatial multiplexing [2], which is well-established in wireless communications [3]. Nowadays several novel techniques such as Mode Group Diversity Multiplexing (MGDM) [4] or Multiple-Input Multiple-Output (MIMO) are in the focus of interest [5].

Among these techniques, optical MIMO has shown its capability for high-speed data transmission. However, the practical implementation has to cope with many technological obstacles such as mode multiplexing and management. This includes mode combining, mode maintenance and mode splitting.

In order to investigate these effects in a whole transmission system a MIMO testbed has been set up. Here, fusion couplers are used for mode combining and splitting in order to realize parallel data transmission over a 1.9 km multi-mode fibre (MMF) [6, 7, 8]. For

the necessary implementation of the MIMO signal processing an off-line MIMO receiver has been programmed.

Against this background the novelty of this paper is the development of a modified MIMO system model by evaluating signals measured within an optical (2×2) MIMO testbed. Its proper mode of operation is shown by the eye diagram.

The remaining part of the paper has the following structure: An introduction of the optical MIMO and its corresponding system model are given in Section 2. In Section 3 the optical MIMO testbed with its components and a testbed-related MIMO system model is described. The obtained results are given in Section 4. Finally, the concluding remarks are shown in Section 5.

2 Optical MIMO System Model

The principle of optical MIMO is based on the excitation of different modes or mode groups. The excitation of different modes or mode groups is realized by mode transformers. In our testbed centric and eccentric splices are used to produce low order modes (LOM) and high order mode (HOM) groups which are combined by a fusion coupler. Subsequently, these different modes travel together in a multi-mode fibre (MMF) and can be separated by their spatial distribution at the receiver side. Fig. 1 illustrates a corresponding electrical MIMO system model. Measurement results of these impulse responses are described in [7].

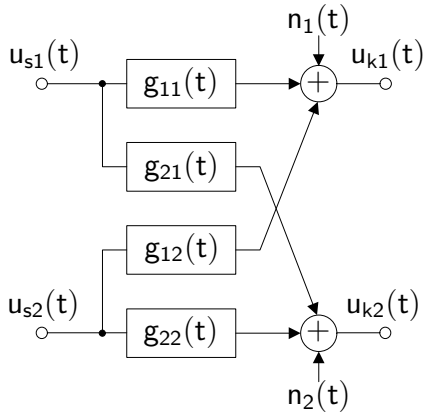

Fig. 1: (2×2) MIMO system model

Here, the mapping of the n_T transmit signals $u_{\mathrm{s}\mu}(t)$ (for $\mu = 1, \ldots, n_\mathrm{T}$) to the n_R received signals $u_{\mathrm{k}\nu}(t)$ (for $\nu = 1, \ldots, n_\mathrm{R}$) is made by using the corresponding impulse responses $g_{\nu\mu}(t)$. Additionally, white Gaussian noise $n_\nu(t)$ (for $\nu = 1, \ldots, n_\mathrm{R}$) is added at the receiver side. Mathematically, the received signals can be described as

$$u_{\mathrm{k}\nu}(t) = \sum_{\mu=1}^{n_\mathrm{T}} u_{\mathrm{s}\mu}(t) * g_{\nu\mu}(t) + n_\nu(t) \tag{1}$$

In this paper the number of transmitters and receivers is limited to $n_\mathrm{T} = n_\mathrm{R} = 2$.

After the receive filtering with $g_{\mathrm{ef}}(t)$ the implementation of the subsequent receiver components such as symbol clock recovery, channel estimation, frame synchronisation and equalisation is carried out as shown in Fig. 2.

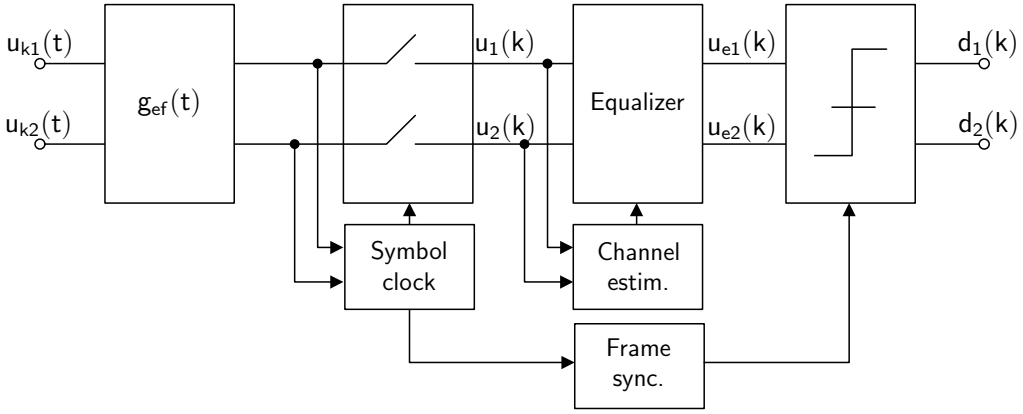

Fig. 2: Receiver component implementation

Here, symbol clock recovery is realized by squaring the received signal. The cross correlation function between the training sequence and the data stream is calculated for the estimation of channel coefficients $h_{\nu\mu}(k)$ (for $\nu = 1, \ldots, n_{\mathrm{R}}$) and (for $\mu = 1, \ldots, n_{\mathrm{T}}$). Furthermore, the resulting cross correlation peak is used for frame synchronisation. With the gained channel coefficients the equalizer coefficients $f_{\nu\mu}(k)$ can be determined by the method of van Etten [9]. Fig. 3 illustrates the equalization of the filtered and sampled receive signals $u_{\nu}(k)$.

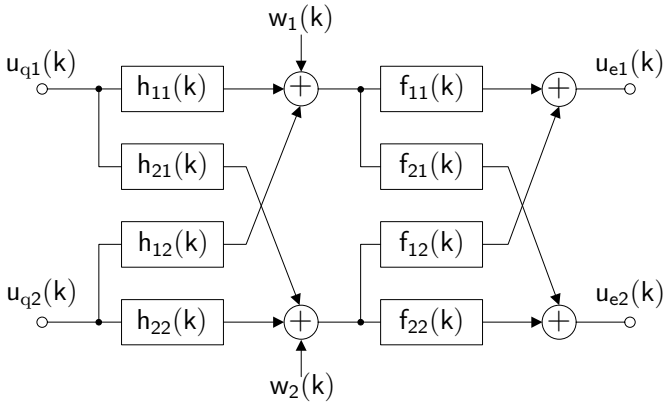

Fig. 3: Structure of the applied ZF-equalization

3 Testbed for MIMO and Data Transmission

In the following, the optical (2×2) MIMO testbed is described. Furthermore, measured signals will be evaluated and a testbed-related model can be developed. With this model it is possible to study the individual receiver components by applying different synthetic data.

3.1 Testbed Implementation

The implementation of the optical MIMO principle within the testbed is constructed as shown in Fig. 4.

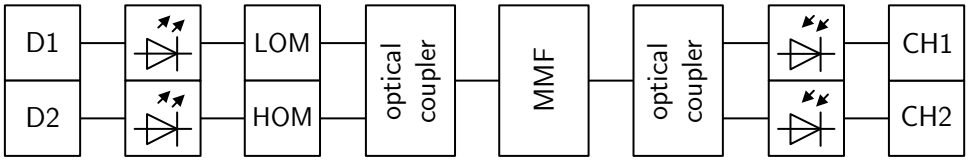

Fig. 4: Structure of the optical (2×2) MIMO transmission system

Here, unipolar signals are generated by two independent data sources (D1, D2) realized by an Agilent high-speed pattern generator N4903B. It also drives the respective electro optical converters (E/O) with a pulse frequency of $f_{\mathrm{T}} = 625$ Mbit/s. The E/O converters consist of lithium niobate modulators and laser diodes operating at a wavelength of 1326 nm. The excitation of the different mode groups (LOM, HOM) is carried out by a centric or an eccentric splice between a single-mode fibre (SMF) and a MMF. To compensate the losses of HOM the higher powered laser diode is used for excitation. Thereafter LOM and HOM are combined by the fusion coupler as shown in [6]. Accordingly fusion couplers can be used on the transmitter side as well as on the receiver side. Thus, after the fibre length of 1.9 km, the transmitted signals are separated by the second fusion coupler followed by two broadband Agilent 81495A receivers (O/E). The obtained signals are sampled by a high-speed sampling oscilloscope (Agilent DSO90804A) and stored for further off-line signal processing (CH1, CH2). The practical set up is shown in Fig. 5.

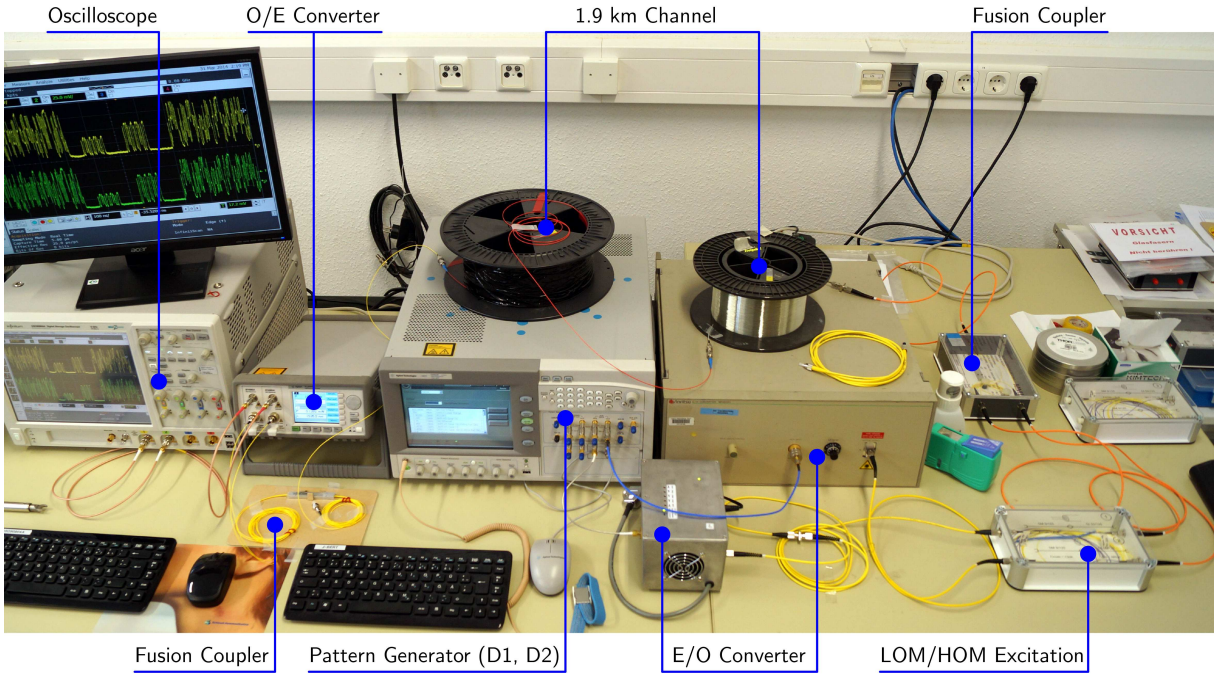

Fig. 5: Setup of the practical (2×2) MIMO system

The developed frame structure is shown in Tab. 1. The payload data are packed into 1024-bit long frames. Each frame consists of 784 bit payload (R), 188 zeros (0) as guard

interval to compensate delay times and a 52 bit training sequence (T), which includes two 26 bit long GSM training sequences.

Table 1: Frame structure consisting of training sequence (T), guard intervals (0) and data (R)

D1 (LOM)	T	T	0	0	0	0	0	0	R	0
D2 (HOM)	0	0	0	0	T	T	0	0	R	0
bit	26	26	26	26	26	26	26	26	784	32
	⟵				1024 bit				⟶	

Referring to Fig. 1, the MIMO channel can be divided into four individual single-input single-output (SISO) channels. The measured receive signals $u_{\mathrm{k}\nu\mu}$ are illustrated in Fig. 6. In each subfigure a relevant portion of the frame including the training sequence and guard interval is shown. This structure is used for the subsequent channel estimation.

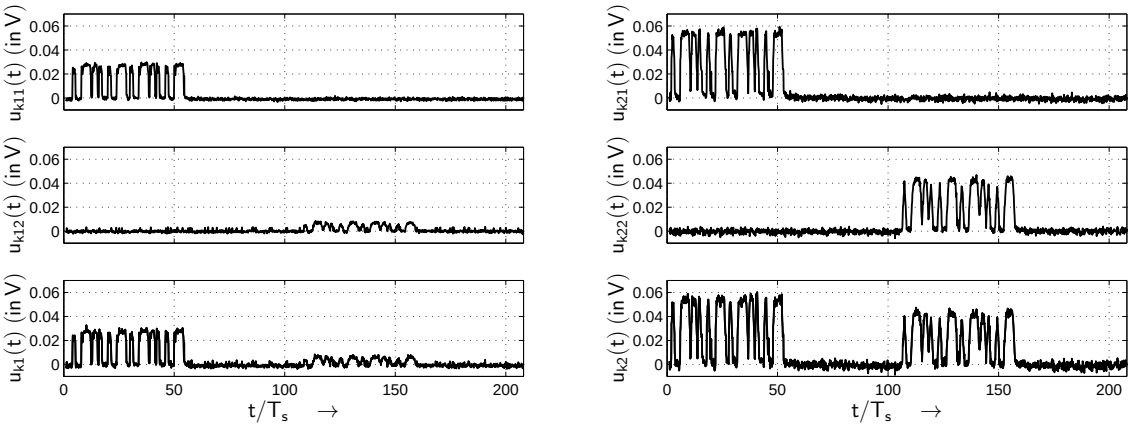

Fig. 6: Frame structure of the measured receive signals $u_{\mathrm{k}1}(t)$ and $u_{\mathrm{k}2}(t)$ (in parts) within the (2×2) MIMO system including training sequence and guard intervals with respect to the pulse frequency $f_{\mathrm{T}} = 1/T_{\mathrm{s}} = 625$ MHz and a fibre length 1.9 km

In comparison to the frame structure shown in Tab. 1 a time delay $\Delta\tau_2$ of 9.2 ns (this corresponds to 5.75 symbols at a pulse frequency $f_{\mathrm{T}} = 1/T_{\mathrm{s}} = 625$ MHz) between the respective transmitted training sequence and the crosstalk has been found. This is caused by different fibre lengths between the data sources and coupler inputs.

3.2 Testbed-related MIMO System Model

Further investigations show a time delay $\Delta\tau_1$ of 3.2 ns (this corresponds to two symbols at a pulse frequency $f_{\mathrm{T}} = 1/T_{\mathrm{s}} = 625$ MHz) between the measured receive signals $u_{\mathrm{k}1}(t)$ and $u_{\mathrm{k}2}(t)$ (Fig. 1). Fig. 7 illustrates the measured receive signals $u_{\mathrm{k}1}(t)$ and $u_{\mathrm{k}2}(t)$. In each subfigure a relevant portion of the frame including the training sequence and guard interval is shown. For a better understanding of the time delay $\Delta\tau_1$ between $u_{\mathrm{k}1}(t)$ and $u_{\mathrm{k}2}(t)$ a detailed illustration of the trainings sequence in $u_{\mathrm{k}1}(t)$ and its crosstalk in $u_{\mathrm{k}2}(t)$ is highlighted in Fig. 8.

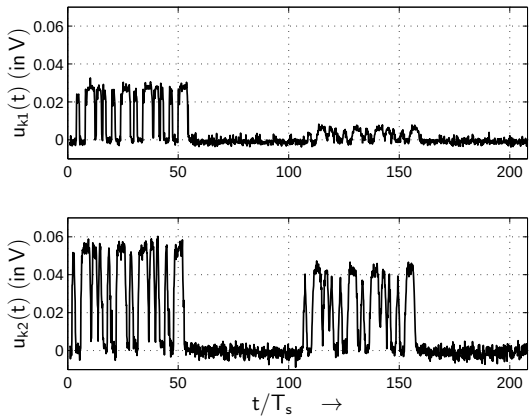

Fig. 7: Frame structure of the measured receive signals $u_{\mathrm{k1}}(t)$ and $u_{\mathrm{k2}}(t)$ (in parts) within the (2×2) MIMO system including training sequence and guard intervals with respect to the pulse frequency $f_{\mathrm{T}} = 1/T_{\mathrm{s}} = 625$ MHz and a fibre length 1.9 km

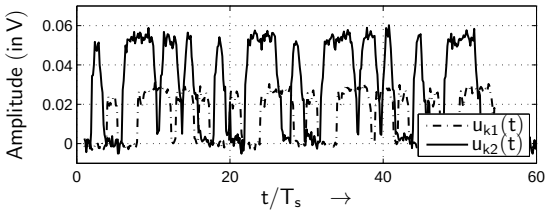

Fig. 8: Time delay $\Delta\tau_1$ between the measured receive signals $u_{\mathrm{k1}}(t)$ and $u_{\mathrm{k2}}(t)$ within the (2×2) MIMO system with respect to the pulse frequency $f_{\mathrm{T}} = 1/T_{\mathrm{s}} = 625$ MHz and a fibre length 1.9 km

Taking into account the time delays $\Delta\tau_1$ and $\Delta\tau_2$ obtained in the (2×2) MIMO testbed, a modified system model is derived as shown in Fig. 9.

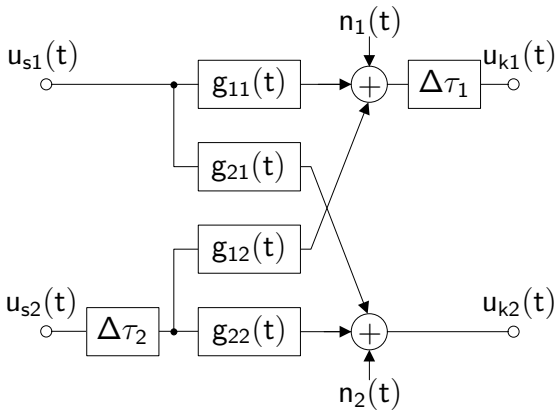

Fig. 9: Testbed-related (2×2) MIMO system model

Here, the n_{T} transmit signals $u_{\mathrm{s}\mu}(t)$ (for $\mu = 1, \ldots, n_{\mathrm{T}}$) are mapped to the n_{R} receive signals $u_{\mathrm{k}\nu}(t)$ (for $\nu = 1, \ldots, n_{\mathrm{R}}$) by using the corresponding impulse responses $g_{\nu\mu}(t)$ and the respective time delays $\Delta\tau_1$ and $\Delta\tau_2$. Additionally, white Gaussian noise $n_\nu(t)$ (for $\nu = 1, \ldots, n_{\mathrm{R}}$) is added at the receiver side.

To investigate the previously determined effects a Simulink model which corresponds to the testbed-related system model in Fig. 9 has been developed for generating synthetic

data. These data are used for subsequent study of the receiver components.

4 Results

In this section the different receiver components are evaluated by taking the before hand measured time delays $\Delta\tau_1 = 3.2$ ns and $\Delta\tau_2 = 9.2$ ns into account. It is worth noting that the time delay $\Delta\tau_1$ can easily be compensated by the frame synchronisation. Therefore only the time delay $\Delta\tau_2$ remains for further consideration.

4.1 Simulation Results

In this section the impact of $\Delta\tau_2$ is studied by a computer simulation. For this simulation the channel impulse responses $g_{\nu\mu}(t)$ (for $\nu = 1, 2$ and $\mu = 1, 2$) are exemplary assumed as:

$$g_{11}(t) = \frac{2}{5}\delta(t) + \frac{1}{5}\delta(t - T_\mathrm{s}) \qquad g_{12}(t) = \frac{3}{10}\delta(t) + \frac{1}{10}\delta(t - T_\mathrm{s})$$
$$g_{21}(t) = \frac{3}{10}\delta(t) + \frac{1}{10}\delta(t - T_\mathrm{s}) \qquad g_{22}(t) = \frac{1}{2}\delta(t) + \frac{1}{10}\delta(t - T_\mathrm{s}) \quad . \qquad (2)$$

For different values of $\Delta\tau_2$ the respective channel impulse responses have been estimated as given in Fig. 10 and Fig. 11. Here the influence of the time delay is clearly visible in the impulse responses $h_{21}(k)$ and $h_{22}(k)$.

The remaining interferences within as well as between the data streams can easily be removed by further signal processing such as the proposed zero forcing (ZF) equalizer as shown in [7].

4.2 Measured Data

In this section the findings from the simulative study are applied. The resulting channel coefficients $h_{\nu\mu}(k)$ from the measured data are illustrated in Fig. 12.

Taking the estimated channel coefficients into account, the ZF equalization can be realized. The corresponding eye diagram is shown in Fig. 13 for the equalized signal $u_{\mathrm{e}1}(t)$.

5 Conclusion

In this contribution an adequate system model describing the practical setup of a (2×2) MIMO testbed has been developed. The corresponding receiver components have been successfully tested by computer simulations as well as by using real data.

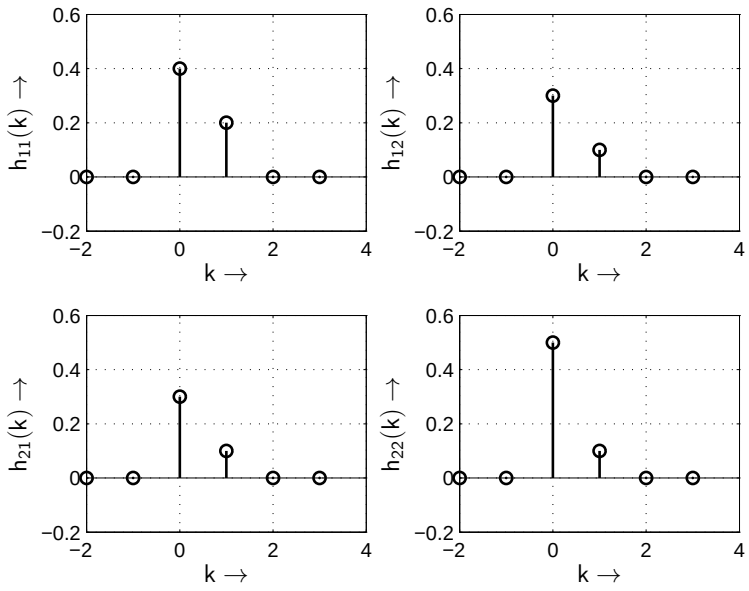

Fig. 10: Estimated channel coefficients of the synthetic receive signal of the (2×2) MIMO Simulation assuming a pulse frequency of $f_{\mathrm{T}} = 1/T_{\mathrm{s}} = 625$ MHz and $\Delta\tau_2 = 0$

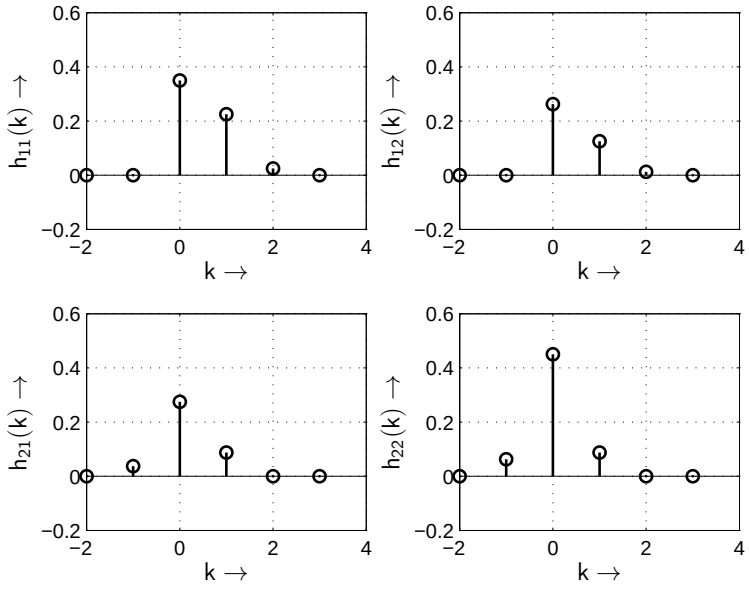

Fig. 11: Estimated channel coefficients of the synthetic receive signal of the (2×2) MIMO Simulation assuming a pulse frequency of $f_{\mathrm{T}} = 1/T_{\mathrm{s}} = 625$ MHz and $\Delta\tau_2 = 9.2$ ns

References

[1] P. J. Winzer. Optical Networking Beyond WDM. *IEEE Photonics Journal*, 4(2):647–651, 2012.

[2] D. J. Richardson, J. Fini, and L. Nelson. Space Division Multiplexing in Optical Fibres. *Nature Photonics*, 7:354–362, 2013.

[3] D. Tse and P. Viswanath. *Fundamentals of Wireless Communication*. Cambridge, New York, 2005.

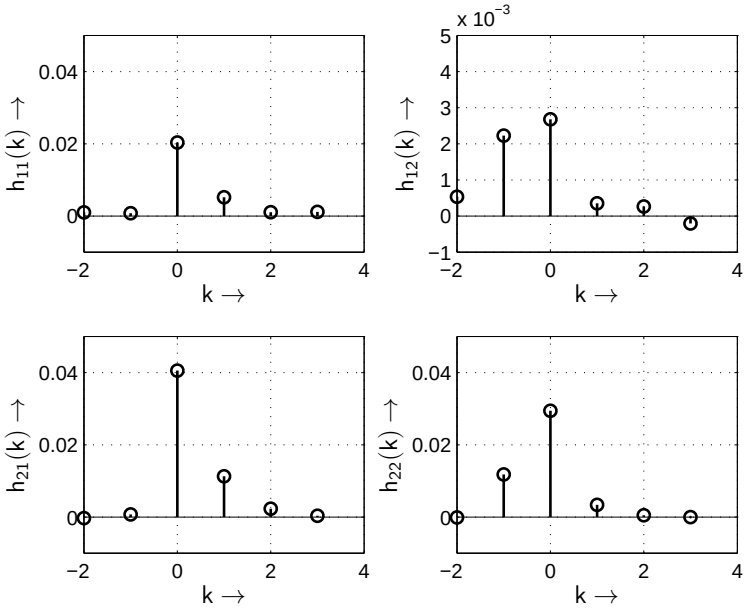

Fig. 12: Estimated channel coefficients of the measured received signal of the (2×2) MIMO Simulation assuming a pulse frequency of $f_\mathrm{T} = 1/T_\mathrm{s} = 625$ MHz

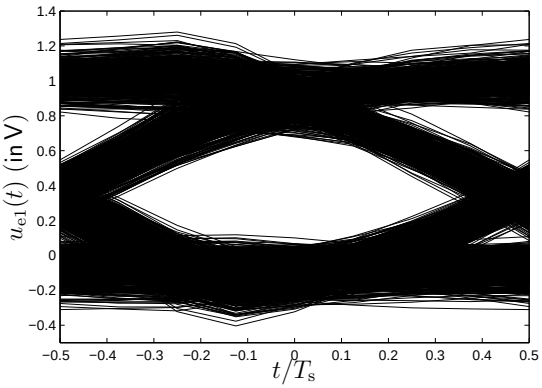

Fig. 13: Eye diagram of measured receive signal $u_{\mathrm{e}1}(t)$ after equalization

[4] B. Franz and H. Bülow. Experimental Evaluation of Principal Mode Groups as High-Speed Transmission Channels in Spatial Multiplex Systems. *Photonics Technology Letters, IEEE*, 24(16):1363–1365, Aug 2012.

[5] A. C. Singer, N. R. Shanbhag, and Hyeon-Min Bae. Electronic Dispersion Compensation – An Overwiew of Optical Communications Systems. *IEEE Signal Processing Magazine*, 25(6):110–130, 2008.

[6] A. Ahrens and S. Lochmann. Optical Couplers in Multimode MIMO Transmission Systems - Measurement Results and Performance Analysis. In *International Conference on Optical Communication Systems (OPTICS)*, pages 398–403, Reykjavik (Iceland), 29.–31. July 2013.

[7] A. Sandmann, A. Ahrens, and S. Lochmann. Equalisation of Measured Optical MIMO Channels. In *International Conference on Optical Communication Systems (OPTICS)*,

pages 37–44, Vienna (Austria), 28.–30. August 2014.

[8] A. Sandmann, A. Ahrens, and S. Lochmann. Experimental Description of Multimode MIMO Channels utilizing Optical Couplers. In *15. ITG-Fachtagung Photonische Netze – ITG-Fachbericht Band 248*, pages 125–130, Leipzig (Germany), 05.–06. May 2014.

[9] W. van Etten. An Optimum Linear Receiver for Multiple Channel Digital Transmission Systems. *IEEE Transactions on Communications*, 23(8):828–834, 1975.